Hierarchical ZSM-5 Catalysts: The Effect of Different Intracrystalline Pore Dimensions on Catalyst Deactivation Behaviour in the MTO Reaction

Tobias Weissenberger,*[a] Albert G. F. Machoke,[a] Jürgen Bauer,[b] Ralf Dotzel,[b] John L. Casci,[c] Martin Hartmann,[d] and Wilhelm Schwieger[a, d]

Abstract: We present the effect of different combinations of intracrystalline pore systems in hierarchical ZSM-5 zeolites on their performance as MTO catalysts. We prepared ZSM-5 zeolites with additional intracrystalline mesoporous, intracrystalline macropores and a novel ZSM-5 type zeolite with intracrystalline meso and macropores. The catalytic results showed that both used catalysts with mesopores and macropores exhibited three times longer catalyst lifetime compared to a conventional catalyst. However, TGA analysis of the deactivated catalysts showed much larger coke content in the mesoporous catalyst than in the macroporous catalyst. Consequently, macro-

pores predominantly led to reduced coke formation rate while additional mesopores predominantly enhanced the resistance against deactivation by coke. Combining both intracrystalline meso and macropores in one catalyst lead to a tenfold increase in catalyst lifetime. Besides the effect on the catalyst lifetime there was also a strong effect of the additional pore systems on the selectivity of the catalysts. The catalysts containing mesopores showed reduced selectivity to short chain olefins and increased selectivity to larger hydrocarbons in comparison to the catalysts without a mesopores system.

Introduction

Zeolites belong to the most important catalytic materials and find widespread application as heterogeneous catalysts for crude oil refining as well as for processes in petro chemistry and fine chemistry.[1] The crystalline framework of zeolites gives rise to micropores with diameters ranging from 0.3 to 1.2 nm. This pore diameters, similar to the dimensions of molecules, give rise to the unique shape selective properties of zeolite catalysts.[2]

While the well-ordered micropore system of zeolites has many advantages, the diffusion coefficients of molecules in the micropores are very low.[3]

Thus, the utilisation of zeolites in catalysis is often limited by slow diffusion of reactant species to the active sites confined within the micropores and diffusion of products out of the micropore system. These diffusion limitations result in reduced utilisation of the zeolite crystal and can also led to reduced selectivity or lifetime of zeolite catalysts.[4] In order to reduce or eliminate these transport restrictions, it is desirable to reduce the diffusion path length within the zeolitic micropores, by either reducing the crystal dimensions (preparation of nano-sized zeolites) or by introduction of an additional larger pore system into the zeolite.[5] The second approach results in hierarchically structured zeolites which consist of at least one additional larger pore system interconnected to the zeolitic micropores.[5a,6]

Hierarchically structured zeolites already showed superior mass transport properties in comparison to conventional purely microporous zeolites.[7] Resulting in enhanced catalytic performance in a number of test reactions such as e.g. catalytic cracking,[8] alkylation,[9] catalytic fast pyrolysis[10] and methanol to hydrocarbon conversion.[11]

Especially the conversion of methanol to hydrocarbons (MTH) benefits greatly from the improved mass transport properties of hierarchical zeolites.

The conversion of synthesis gas (H$_2$, CO short Syngas), produced from biomass, coal or natural gas, to hydrocarbons is of great interest since it could be used to provide olefins and fuels from non-oil feedstock.[12] An established process for the conversion of syngas to hydrocarbons is the Fischer-Tropsch process using e.g. Co or Fe based catalysts.[13] However, the

[a] Dr. T. Weissenberger, Dr. A. G. F. Machoke, Prof. W. Schwieger
     Institute of Chemical Reaction Engineering
     University of Erlangen-Nuremberg
     Egerlandstr. 3
     91058 Erlangen (Germany)
     E-mail: tobias.weissenberger@fau.de
[b] Dr. J. Bauer, Dr. R. Dotzel
     Johnson Matthey Catalysts (Germany) GmbH
     Bahnhofstr. 43
     96257 Redwitz (Germany)
[c] Dr. J. L. Casci
     Johnson Matthey Technology Centre
     PO Box 1, Belasis Avenue
     Billingham, TS23 1LB (UK)
[d] Prof. M. Hartmann, Prof. W. Schwieger
     Erlangen Catalysis Resource Center
     University of Erlangen-Nuremberg
     Egerlandstr. 3
     91058 Erlangen (Germany)

conversion of syngas to methanol followed by conversion of the methanol to hydrocarbons (MTH) over acidic zeolite or zeotype catalysts can increase the product selectivity.[14] The MTH reactions are therefore promising processes for the upgrading of methanol to value added products such as olefins (MTO), gasoline (MTG) and propene (MTP).[15] Unfortunately the catalysts are rapidly deactivated by deposition of coke within the channels and cages or on the external surface of the zeolite and subsequent blocking of the zeolitic micropores.[16] This catalyst deactivation makes a periodical regeneration of the catalyst by oxidation of the accumulated coke necessary.

Hierarchical zeolites can facilitate a fast and effective removal of larger hydrocarbons, which often act as coke precursor species, and thus reduce coke formation and catalyst deactivation.[17] Beside this, many hierarchical zeolites also offer a larger external surface area (e.g. due to mesopores) which increases the resistance against deactivation by the deposited coke.[18]

Thus, hierarchically structured ZSM-5 zeolites (MFI topology) could already demonstrate drastically increased catalyst lifetimes in comparison to conventional, purely microporous zeolite catalysts in the MTH reaction.[19] However, until now, the focus of these studies was on mesoporous catalysts prepared by desilication or soft templating approaches.[18,20]

While mesoporous ZSM-5 catalysts have been studied extensively, very little is known about the effect of additional macropores. Li et al. prepared a ZSM-5 catalyst with a small degree of additional macroporosity and studied the catalytic performance in MTO. However, the studied catalyst also contained mesopores, making a differentiation of the effects of meso and macropores challenging.[21] We could recently show that additional intracrystalline macropores drastically enhance the catalyst lifetime of ZSM-5 catalysts in the MTO reaction by reducing the coke formation.[22]

In this work we compare the MTO performance of catalysts with different combinations of pore systems: purely microporous, micro/mesoporous, micro/macroporous and micro/meso/macroporous with focus on coke formation and deactivation behaviour.

For the investigations, four ZSM-5 catalysts with similar bulk properties were prepared: a) a conventional ZSM-5 catalyst used as reference, prepared by hydrothermal synthesis, b) a hierarchically structured ZSM-5 zeolite with intracrystalline mesopores prepared by alkaline treatment, c) a hierarchically structured ZSM-5 zeolite with large intracrystalline macropores prepared by inverse crystallisation of mesoporous silica spheres and d) a ZSM-5 zeolite with both intracrystalline meso and macropores prepared by alkaline treatment of an macroporous ZSM-5 zeolite. These catalysts were characterised and tested in the MTO reaction under the same reaction conditions.

Results and Discussion

Catalyst characterisation

For the study four different catalysts were prepared and characterised. A conventional ZSM-5 zeolite and a macroporous ZSM-5 zeolite were synthesised using hydrothermal and steam assisted crystallisation. A fraction of these samples was then subsequently alkaline treated to generate additional intracrystalline mesopores. So four different samples were obtained: a) purely microporous, conventional ZSM-5 zeolite, b) mesoporous ZSM-5 c) macroporous ZSM-5 zeolite and d) macro/mesoporous ZSM-5 zeolite.

The diffraction patterns of the synthesised parent conventional and macroporous zeolite samples, shown in Figure 1, were typical for MFI zeolites. All pattern showed only MFI typical reflections and no indication for the presence of phase impurities. After alkaline treatment a small reduction in XRD intensities were evident, which indicates a loss of crystallinity. The decrease in crystallinity of the alkaline treated samples is also evident in the calculated relative crystallinities, shown in Table 1, which decreased during alkaline treatment by 15 and
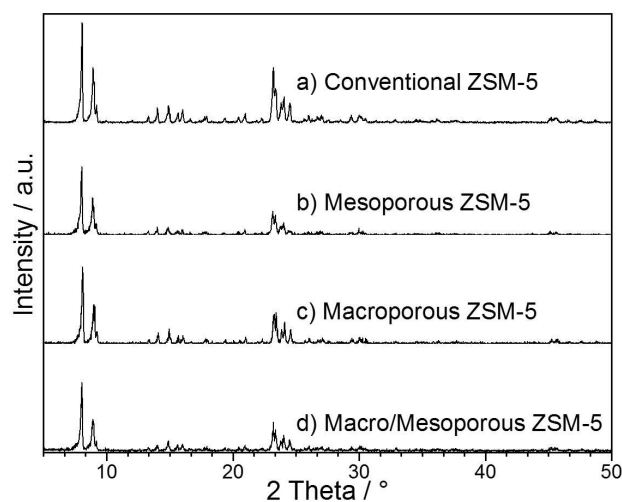

Figure 1. Powder XRD patterns of the different studied ZSM-5 zeolite catalysts.

Table 1. Nitrogen sorption data of the used hierarchical ZSM-5 catalysts.

	a) Conv.	b) Meso	c) Macro	d) Macro/Meso
Si/Al[a] mol mol^{-1}	111	106	108	101
$C_{Brønsted}$[b] µmol g^{-1}	188	187	190	186
V_{Micro}[c] cm^3 g^{-1}	0.17	0.13	0.18	0.12
V_{Total}[d] cm^3 g^{-1}	0.225	0.350	0.261	0.391
S_{BET}[e] m^2 g^{-1}	419	418	431	436
S_{Extern}[f] m^2 g^{-1}	28.6	121.9	35.0	183.0
HF[g] –		0.049	0.079	0.051	0.100

[a] Measured by ICP-OES, [b] Measured by NH$_3$-TPD, [c] t-plot method micropore volume. [d] DFT-method cumulative pore volume. [e] BET specific surface area. [f] t-plot method external surface area. [g] Hierarchy Factor calculated as reported by Pérez-Ramírez et al.[27]

ChemCatChem

Full Papers
doi.org/10.1002/cctc.201902362

Chemistry Europe
European Chemical
Societies Publishing

18% for the conventional and macroporous ZSM-5 zeolites, respectively.

The obtained conventional ZSM-5 zeolite, prepared by hydrothermal synthesis, showed MFI typical coffin shaped crystals with an average crystal length of about 700 nm (see Figure 2). The synthesised macroporous zeolite consisted of crystals with an average length of around 3 micron and macropores were visible on the crystal surface. The macropores were between 200 and 500 nm in diameter and exhibited an average diameter, estimated by SEM, of about 360 nm.

The mesoporous ZSM-5 sample prepared by alkaline treatment of the conventional zeolite showed non altered crystal dimensions and crystal shape compared to the conventional ZSM-5 zeolite.

The macro/mesoporous ZSM-5 sample prepared by alkaline treatment of the macroporous sample also retained the crystal shape and dimensions. Furthermore the intracrystalline macropores were not affected by the alkaline treatment, thus the sample shows the same average macropore diameter as the parent macroporous zeolite. Worth mentioning are some remains of the MSPs used as sacrificial template for the synthesis of the macroporous zeolite which are still visible in the SEM images of the sample (Figure 2 c). These residual MSPs were not visible in the SEM images of the macro/mesoporous

Figure 2. SEM images of a) conventional ZSM-5, b) mesoporous ZSM-5, c) macroporous ZSM-5 and d) macro/mesoporous ZSM-5.

Figure 3. Nitrogen sorption isotherms of the different studied ZSM-5 catalysts, samples mesoporous ZSM-5 and macro/mesoporous ZSM-5 plotted with an off set of 150 cm³ g⁻¹.

zeolite sample. It is very likely that the amorphous MSPs residues were dissolved early in the alkaline treatment process.

Nitrogen sorption measurements proved the generation of additional mesopores during the alkaline treatment (Figure 3). The isotherms of the conventional and macroporous ZSM-5 samples were of IUPAC type I, characteristic for microporous materials. After alkaline treatment both samples showed type IV isotherms, which are characteristic for micro/mesoporous materials.[25] In contrast to the mesoporous sample, the macro/mesoporous sample showed adsorption at lower relative pressure indicating the presence of small mesopores.

The textural properties of the catalyst are shown in Table 1. The conventional and the macroporous catalyst showed values for BET surface area and micropore volume typical for purely microporous MFI type zeolites, which is in good accordance with the observed high crystallinity of these samples.

The mesoporous zeolite showed increased external surface area and total pore volume, while the micropore volume decreased during the alkaline treatment. Similar trends were observed for the macro/mesoporous zeolite. However, the generation of mesopores by alkaline treatment was slightly more effective for the macroporous ZSM-5 zeolite than for the conventional ZSM-5 and resulted in higher mesoporosity and higher external surface area but also in further reduced micropore volume. The higher effectiveness of the alkaline treatment might be caused by the slightly higher external surface area of the parent macroporous zeolite compared to the conventional zeolite.

Again, the reduced micropore volume of the mesoporous and macro/mesoporous zeolites are in good accordance with the lower intensity observed by using XRD. The reduced crystallinity and micropore volume of alkaline treated zeolites is well known in the literature.[24,26] The pore size distribution (Supporting information Figure-ESI-1) reveals that small mesopores between 2 and 20 nm were generated by the alkaline treatment. Again, the slightly more effective mesopores generation for the macroporous zeolite is observable in the pore size distribution.

The hierarchy factor (HF) of all four samples was calculated as reported by Pérez-Ramírez and co-workers.[27] and is given in Table 1. The hierarchy factor compares the relative mesoporous surface area (calculated using S_{meso}/S_{BET}) and the relative micropore volume ($V_{micro}/V_{total, p/p0} = 0.99$) of the sample. Therefore, the hierarchy factor is not applicable for hierarchical zeolites with macropores. The hierarchy factor of the conventional ZSM-5 sample and the macroporous zeolites were relatively low, since both samples do not contain mesopores. The hierarchy factors of the mesoporous catalysts were higher with values of 0.07 and 0.1 for the mesoporous ZSM-5 zeolite and the macro/mesoporous ZSM-5 zeolite, respectively. The higher HF of the macro/mesoporous zeolite can be attributed to higher mesopore volume due to more effective alkaline treatment. The obtained HF-values are comparable to values of hierarchically structured zeolites prepared using post synthetic alkaline treatment found in the literature.[27] However, one must keep in mind that the additional macropores are not considered in the hierarchy factor.
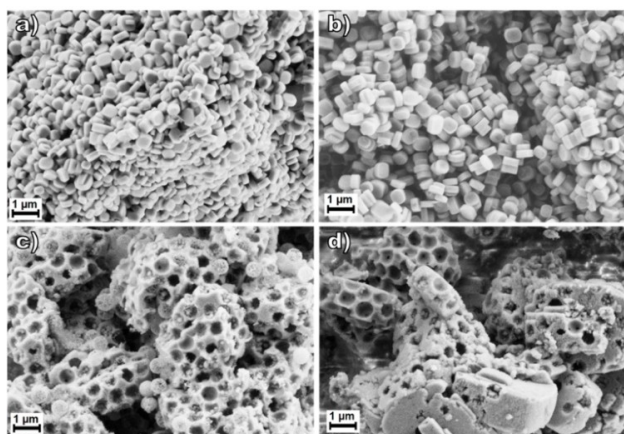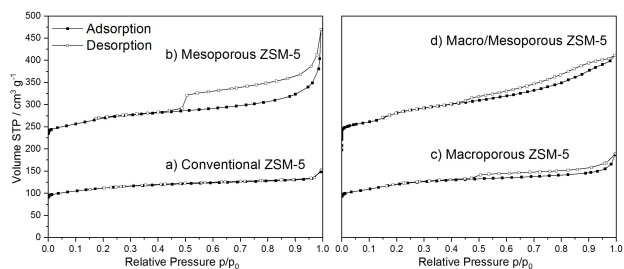
The chemical compositions of all prepared samples were comparable as evident by similar Si/Al ratios measured by ICP-OES (see Table 1). A slight decrease in the Si/Al ratios was evident for alkaline treated samples. This increase in aluminium content indicates a higher silicon removal compared to aluminium removal.

The number of Brønsted acid sites, determined by NH_3-TPD, was also comparable for all zeolite samples. All samples showed values around 180 μmol desorbed ammonia per gram of zeolite in H-form. The constant number of Brønsted acid sites but slightly higher aluminium content of the alkaline treated samples might be caused by the formation of extra framework aluminium species during the alkaline treatment. However, both the differences in Brønsted acid sites and chemical composition are very small.

The presented NH_3-TPD data does not give information about the distribution of the acid sites. Since the different used synthesis methods and post-synthetic treatments might alter the distribution of acid sites, future detailed investigations of the acid site distribution and surface acidity would give important additional information about the zeolite properties.

In summary, zeolites with similar bulk characteristics but different additional intracrystalline pore-systems (no additional pores, mesopores, macropores and macro and mesopores) have been prepared using different techniques.

Catalytic performance in the MTO reaction

MTO performance of the different catalysts was evaluated under the same conditions. 50 ml min^{-1} Helium, saturated with methanol at 303 K, was passed through 100 mg of the catalyst at 723 K resulting in a WHSV of 11 $g_{Methanol} g_{catalyst}^{-1} h^{-1}$. The products were analysed by using an online GC-FID. For the conversion calculations, dimethyl ether (DME) was treated as a reactant rather than a product.

The observed catalysts lifetimes of the zeolites differed drastically when different additional pore systems were present in the catalysts as visible in conversion of methanol and dimethyl ether over time on stream in Figure 4.

The conversion of the conventional ZSM-5 catalyst declined rapidly after 8 hours on stream, resulting in a complete loss of catalytic activity after just 12 hours.

The deactivation of the mesoporous and the macroporous ZSM-5 catalysts was slowed down drastically by their corresponding additional pore system. In contrast to the conventional catalyst, the mesoporous and macroporous catalysts showed an extended period of complete conversion of 18 and 21 h time on stream, respectively.

The deactivation of the mesoporous catalyst was proceeding slightly slower than observed for the macroporous catalyst. This resulted in comparable lifetimes of the catalysts. The macro/mesoporous catalyst showed complete conversion to 21 h comparable to the macroporous ZSM-5 catalyst. However, the deactivation of the macro/mesoporous catalyst proceeded much slower which resulted in significantly prolonged catalyst lifetime. The catalyst lifetimes to 50% conversion were: conven-
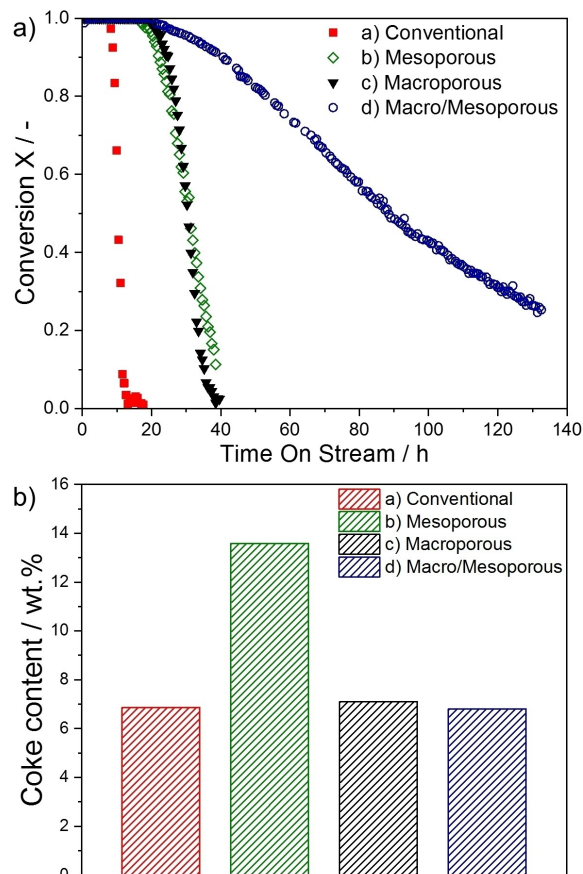

Figure 4. a) Conversion of methanol and DME over time on stream (whsv 11 g g^{-1} h^{-1}, T = 723 K) and b) coke content in the corresponding, spent catalysts measured by TGA after the last point in the conversion graph.

tional ZSM-5 10 h, mesoporous ZSM-5 28 h, macroporous ZSM-5 32 h and macro/mesoporous ZSM-5 78 h.

The coke content in the four spent catalysts, after reaction (measured by TGA after the last point in the conversion graph, Figure 4a), is shown as bars in Figure 4 b). The spent conventional and macroporous ZSM-5 catalysts showed comparable coke content of 6.87 and 7.10 wt.–% after 18 and 39 hours on stream, respectively. However, the deactivated mesoporous ZSM-5 catalyst, after 38 hours on stream, did accumulate almost double the amount of coke as the conventional and the macroporous catalysts. The coke content in the spent catalysts correlates well with the external surface area of the catalysts.

The conventional and macroporous catalysts showed almost the same external surface area and deactivated with very similar coke content. The mesoporous catalyst showed much higher external surface area and consequently accumulated much more coke in comparison to conventional and macroporous catalysts. Those results are in good accordance with the proposed deactivation of ZSM-5 catalysts by accumulation of coke on the external surface area rather than within the micropores.[28]

Considering that the mesoporous and the macroporous catalysts were deactivated more or less after the same time on

ChemCatChem

Full Papers
doi.org/10.1002/cctc.201902362

**Chemistry
Europe**
European Chemical
Societies Publishing

stream but show significant differences in their coke content, their coke formation rate must differ greatly. Assuming linear coke formation over the complete time on stream, the mesoporous catalyst would have nearly double the coke formation rate as the macroporous catalyst. Therefore, the prolongation of the catalyst lifetimes observed for the meso and macroporous catalysts were caused by different effects. Additional macropores predominantly reduced the coke formation during the reaction. Additional mesopores only led to slightly reduced coke formation in comparison to the conventional catalyst but predominantly enhanced the resistance against deactivation by the accumulated coke due to enlarged external surface area.

Both effects led to comparable catalyst lifetime, however the reduced coke formation rate has several advantages. For example the reduced coke formation results in higher selectivity to hydrocarbons and the reduced coke content in the spend catalyst facilitates the regeneration and can therefore reduce the damage caused to the catalyst during the regeneration (e.g. dealumination).

The observed coke content in the spent macro/mesoporous catalyst was around 7 wt.–% and was comparable to the macroporous and conventional catalysts. However, the macro/mesoporous catalyst was not completely deactivated and therefore higher coke accumulation after complete deactivation is likely. Nevertheless, the catalyst is unlikely to accumulate the same coke amount as the mesoporous catalyst after complete deactivation.

Considering the much longer lifetime of the macro/mesoporous catalyst the resulting coke formation per time on stream was significantly lower than the observed for the other tested catalysts. This could be explained by the combination of macropores and mesopores which both contribute to reduced coke formation rate.

In future, it would be interesting to use spatially resolved micro-imaging to investigate the catalytic behaviour and coke formation of zeolites with different textural properties during the reaction.[30]

The selectivity to the desired C_2–C_4 olefins over time on stream shows similar trends as the conversion (see Figure 5). However, the catalysts differed in their initial selectivity to these olefins. The conventional and macroporous catalysts showed high selectivity of 77% while both the mesoporous and the macro/mesoporous catalysts showed a lower selectivity of around 72%. The selectivities of the conventional and macroporous catalysts were initially stable but started to decline after 5 and 9 hours on stream, respectively. In contrast, the selectivity observed for meso and macro/mesoporous catalysts declined right from the beginning of the reaction.

The observed selectivities of the conventional, macroporous and mesoporous catalysts started to drop significantly at the same moment the conversion started to fall below 1. However, this trend was not evident for the macro/mesoporous catalyst which showed a more or less steady decline in selectivity over the complete reaction time.

As already mentioned, the macro/mesoporous catalyst showed a reduced selectivity to short chain olefins in compar-
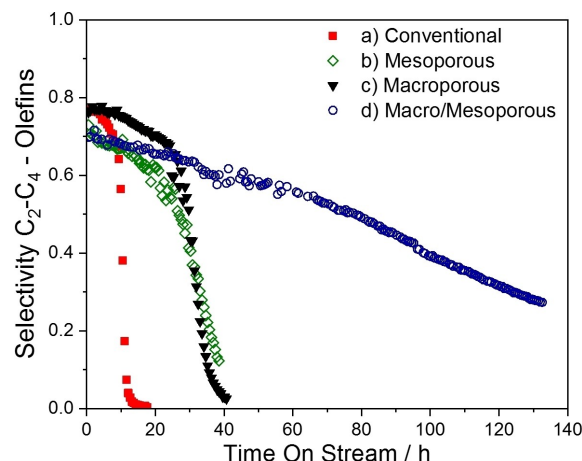
Figure 5. Selectivity to short chain olefins of the different catalysts over time on stream (whsv 11 g g^{-1} h^{-1}, T = 723 K)

ison to the conventional and macroporous catalysts. Nevertheless, the much slower deterioration of the selectivity led to increased total olefin yield over the complete reaction time for the macro/mesoporous catalyst.

The observed initial selectivity of the studied catalysts to different hydrocarbon fractions, shown in Figure 6, revealed significant differences between the mesoporous catalysts (mesoporous and macro/mesoporous ZSM-5) and non-mesoporous catalysts (conventional and macroporous ZSM-5). Both mesoporous catalysts showed an increased selectivity to the C_2 fraction and to larger C_{6+} hydrocarbons in comparison to their parent conventional or macroporous ZSM-5 catalysts. The alkaline treatment further resulted in a decrease in selectivity to the C_3 hydrocarbons by 6%. The selectivity to C_4 and C_5 hydrocarbons was not altered by the alkaline treatment and was maintained for both alkaline treated conventional and macroporous catalysts.
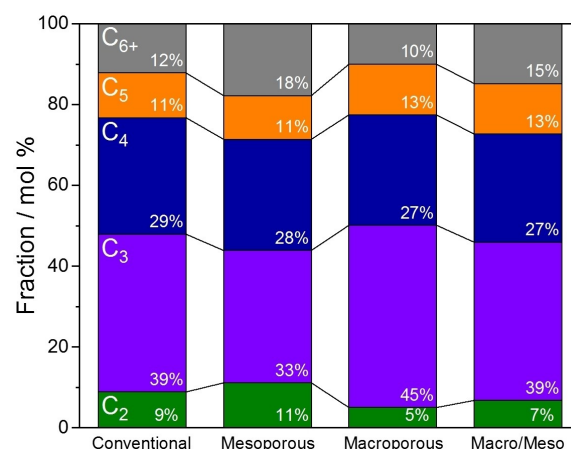
Figure 6. Initial product distribution after 3 h TOS for the different studied catalysts (whsv 11 g g^{-1} h^{-1}, T = 723 K).

ChemCatChem

Full Papers
doi.org/10.1002/cctc.201902362

**Chemistry
Europe**

European Chemical
Societies Publishing

The differences in selectivity between mesoporous and non-mesoporous catalysts might have been caused by the increased external surface area and the decreased crystallinity of the mesoporous catalysts.

Interestingly, the methane concentration over the reaction time represented the deactivation behaviour of the catalysts very well (see Figure 7). An increasing methane selectivity was reported to indicate coke formation, since methane is produced by dehydrogenation of coke species with methanol and thus represents the hydrogen rich by-product of the formation of hydrogen-deficient coke.[28]

The highest coke formation was evident for the conventional catalyst and this catalyst showed the highest methane formation as well. The concentration of methane in the product stream of the conventional catalyst increased very fast and reached its maximum at 8 h time on stream, the same time the conversion started to decline. After this time, the catalyst deactivation inhibited further coke formation, which results in reduced methane formation. The same trend was observed for the mesoporous and macroporous catalysts. The mesoporous and macroporous catalysts both showed increasing methane formation to about 21 and 23 h, respectively. Then the declining conversion led to decreasing methane concentrations in the product streams. While both catalysts showed the same trend, the methane formation overserved for the mesoporous catalyst was higher which is in good accordance to the higher coke content after reaction.

The macro/mesoporous catalyst showed a reduced methane production and a different trend in comparison to the other studied catalysts. The methane concentration in the product stream of the macro/mesoporous catalyst increased very slowly to about 50 h and then decreases again. The conversion graph of the macro/mesoporous catalyst is not S-shaped as observed for the other catalysts but rather a linearly decreasing. This difference in conversion might explain the different methane production over time on stream.

The methane formation is therefore an excellent indicator for coke formation and catalyst lifetime of MTH catalysts and could be used for fast catalyst screening without the need for complete catalyst deactivation.

Conclusions

We could successfully prepare hierarchical ZSM-5 catalysts with different types of additional, intracrystalline pore systems (mesopores, macropores and a combination of both) while keeping the bulk properties constant and use this set of catalysts to study the effect of additional pore systems on the catalytic performance in the MTO reaction. For the first time we could prepare a novel type of macro/mesopore system by a combination of invers crystallisation[29] and post synthetic alkaline treatment.

All hierarchical catalysts showed prolonged catalyst lifetimes in comparison to the conventional, purely microporous ZSM-5 catalyst. The catalyst with intracrystalline mesopores and the catalyst with intracrystalline macropores showed comparable lifetimes, nearly three times longer than the conventional ZSM-5 catalyst. The hierarchical catalyst with an intracrystalline system of both macro and mesopores showed a significantly different catalytic behaviour: A drastically prolonged catalyst lifetime (nearly 10 fold increase of time on stream to $X = 50\%$) and a different course of deactivation.

The different ways mesopores and macropores effect the catalyst deactivation is the other important outcome of this study. The overserved coke formation indicated that additional intracrystalline macropores predominantly reduced the coke formation while additional mesopores mainly increased the catalysts resistance against deactivation by coke due to increased external surface area.

Another interesting finding was the reduced selectivity to short chain olefins and in parallel increased selectivity to larger hydrocarbons in case that mesopores are present in the catalyst. The observed methane production reflected the deactivation behaviour very well and was proven a good indicator for the coke formation and thus for the catalyst deactivation.

In general, we hope that we could demonstrate that intracrystalline macropores, on their own or in combination with mesopores, contribute to drastically enhanced catalytic performance of ZSM-5 catalysts in the MTO reaction.

Experimental Section

Synthesis of conventional ZSM-5 catalyst

Conventional ZSM-5 crystals were prepared by hydrothermal synthesis following our previous reported procedure.[22]

In a typical synthesis, 21.3 g of a $1\,\mathrm{mol\,l^{-1}}$ tetrapropylammonium hydroxide solution (TPAOH, Sigma Aldrich) and 25 g deionised water were stirred in a polypropylene bottle. Then 20 g tetraethylorthosilicate (TEOS, Alfa Aesar) was added dropwise under vigorous stirring. The mixture was stirred for 4 h before 0.36 g aluminium nitrate nonahydrate (Sigma Aldrich) dissolved in 25 g deionised water was added. The mixture was then stirred for one
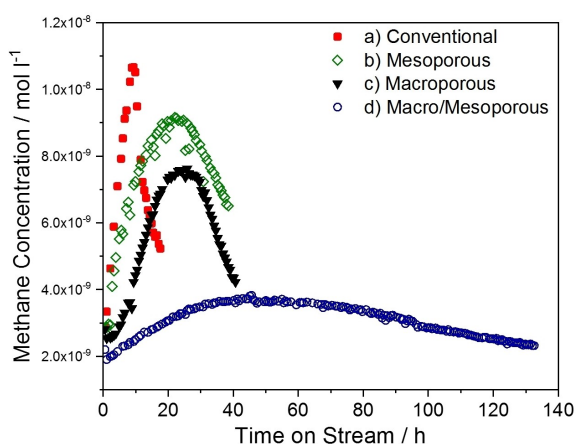
Figure 7. Methane concentration in the product stream over time on stream (whsv $11\,\mathrm{g\,g^{-1}\,h^{-1}}$, $T = 723\,\mathrm{K}$).

ChemCatChem

Full Papers
doi.org/10.1002/cctc.201902362

Chemistry
Europe
European Chemical
Societies Publishing

hour. The hydrothermal synthesis was performance in PTFE-lined stainless steel autoclaves at 448 K for 48 h under static conditions.

After the synthesis, the zeolite sample was recovered by centrifugation, washed with DI water and dried overnight at 348 K.

Synthesis of macroporous ZSM-5 catalyst

Macroporous ZSM-5 zeolite catalysts were prepared following our previously reported procedure using mesoporous, spherical silica particles as sacrificial template.[22]

Spherical mesoporous silica particles (MSPs) were synthesised as reported by Machoke et al.[23] 2264 g ethanol (Merck Emsure) were mixed with 830 g deionised water. Then 6.0 g hexadecyltrimethylammonium bromide (CTAB, >98% Sigma Aldrich) was dissolved in the mixture before 130.4 g 25 wt.–% aqueous ammonia solution (Merck Emsure) was added. The mixture was stirred for 1 h before the synthesis was started by adding 18.8 g tetraethylorthosilicate (TEOS, >99% Sigma Aldrich). The reaction was carried out under stirring (250 rpm) for 2 hours at room temperature. Afterward, the MSPs were recovered by centrifugation, washed three times with DI water and ethanol and then dried overnight at 348 K.

To remove the surfactant the MSPs sample was calcined in a muffle furnace at 823 K for 6 h under air flow (heating ramp $= 1.2$ K min^{-1}).

For the synthesis of macroporous ZSM-5 type zeolite, 1.0 g of the calcined MSPs were mixed with 3.15 g of an aqueous 2 wt.–% aluminium nitrate nonahydrate solution and then dried at 303 K for 3 h. Then the dried powder was mixed with 1.39 g of a 40 wt.–% aqueous tetrapropylammonium hydroxide solution (Sigma Aldrich). Afterward the impregnated MSPs were dried at 313 K for 1.5 h in a convection oven. The dry powder was crushed and transferred into PTFE crucibles. Steam assisted crystallisation was performed in 23 ml Parr autoclaves at 403 K for 72 h. After crystallisation, the zeolite was recovered by filtration, washed extensively with DI water and dried at 348 K for 12 h. To remove the structure-directing agent, all zeolite samples were calcined in a muffle furnace under 300 l h^{-1} airflow at 823 K for 6 hours (heating ramp 1.2 K min^{-1}).

Preparation of mesoporous and macro/mesoporous ZSM-5 catalyst

The mesoporous and macro/mesoporous ZSM-5 type catalysts were prepared by alkaline treatment of the synthesised conventional and macroporous ZSM-5 samples, respectively. The alkaline treatment was performed as reported in the literature by Groen et al.[24]

500 mg of the calcined zeolite sample was stirred in 15 g of 0.2 M aqueous sodium hydroxide solution at 333 K for 30 minutes. After the alkaline treatment, the flask was cooled down using ice water and the solid was recovered by centrifugation and washed with water until a pH of 8 was reached. The samples were dried over night at 348 K.

Ion exchange

The zeolite samples were transferred into ammonium form by three subsequent ion exchange steps with 1 M aqueous ammonium nitrate (Merck Emsure) solution at 338 K for 6 h ($w_{liquid}/w_{solid} = 30$). After each ion exchange step the solid was recovered by centrifugation, washed with water and dried at 348 K.

Before characterisation and catalytic testing, the ammonium form of the zeolite samples were converted into the active proton form by calcination in a muffle furnace under 300 l h^{-1} air flow at 823 K for 4 h (heating ramp 1.2 K min^{-1}).

Catalyst characterisation

Powder XRD patterns were measured by using a Philips diffractometer equipped with a Cu–Kα X-ray-tube (40 kV, 40 mA).

Scanning electron microscopy (SEM) micrographs were taken by using a Carl Zeiss ULTRA 55 microscope at a voltage of 1.5 to 3.0 kV without pre-treatment of the samples.

Nitrogen sorption isotherms were measured at 77 K using a Quantachrom Autosorb SI. Before the physisorption measurements, the samples were degassed at 523 K under vacuum for a duration of 12 h.

Ammonia temperature programmed desorption (NH$_3$-TPD) experiments were carried out using a Porotec TPD/R/O 1100 instrument. Before measurement, the samples were degassed at 873 K under Helium flow for 3 h. Ammonia adsorption was carried out at 393 K for 30 min. Desorption measurements were then carried out by heating the sample to 873 K with a heating ramp of 10 K min^{-1}.

The chemical composition of the samples was measured by ICP-OES using a Spectro Ciros CCD instrument. The samples were digested (microwave assisted, 523 K, 30 min) in a mixture of HCl (37 wt.–%, Merck Emsure), HNO$_3$ (65 wt.–%, Merck Emsure) and HF (40 wt.–%, Merck Emsure) and diluted with deionised water prior the measurements.

Catalytic testing

All MTO reactions were carried out under the same reactions conditions using a continuous flow gas phase catalyst test rig. The catalyst (100 mg) was mixed with silicon carbide (4 g, 47 grid) and placed between two quartz wool beds in a tubular quartz glass reactor. Initially, the catalysts were pre-treated at 723 K (heating ramp 5 K min^{-1}) under 50 ml min^{-1} He flow for one hour. Before the reaction was started, several bypass measurements were taken. For the reaction, 50 ml min^{-1} Helium flow was saturated with methanol at 303 K and passed through the catalyst bed resulting in a weight hourly space velocity of 11 g g^{-1} h^{-1}. The Product stream was analysed every 30 minutes by using a Varian 3900 GC equipped with a 30 m Agilent Plot-Q column and flame ionisation detector. For the conversion calculations, dimethyl ether (DME) was considered a reactant and not a product. The spent catalysts were recovered and separated from the silicon carbide by sieving. The coke content in the spent catalysts was then measured by using TGA.

Conflict of Interest

The authors declare no conflict of interest.

[1] A. Corma, *Chem. Rev.* **1995**, *95*, 559–614.

[2] C. R. Marcilly, *Top. Catal.* **2000**, *13*, 357–366.

[3] J. Kärger, D. Freude, *Chem. Eng. Technol.* **2002**, *25*, 769–778.

[4] J. Perez-Ramirez, C. H. Christensen, K. Egeblad, C. H. Christensen, J. C. Groen, *Chem. Soc. Rev.* **2008**, *37*, 2530–2542.

[5] a) M. Hartmann, *Angew. Chem. Int. Ed.* **2004**, *43*, 5880–5882; b) S. Mintova, J.-P. Gilson, V. Valtchev, *Nanoscale* **2013**, *5*, 6693–6703.

[6] W. Schwieger, A. G. Machoke, T. Weissenberger, A. Inayat, T. Selvam, M. Klumpp, A. Inayat, *Chem. Soc. Rev.* **2016**, *45*, 3353–3376.

[7] D. Schneider, D. Mehlhorn, P. Zeigermann, J. Kärger, R. Valiullin, *Chem. Soc. Rev.* **2016**, *45*, 3439–3467.

[8] a) H. Konno, R. Ohnaka, J. -i Nishimura, T. Tago, Y. Nakasaka, T. Masuda, *Catal. Sci. Technol.* **2014**, *4*, 4265–4273; b) A. Peral, D. Serrano, J. Přech, C. Ochoa-Hernández, J. Čejka, *Catal. Sci. Technol.* **2016**, *6*, 2754–2765.

[9] a) C. H. Christensen, K. Johannsen, I. Schmidt, C. H. Christensen, *J. Am. Chem. Soc.* **2003**, *125*, 13370–13371; b) L. Chen, T. Xue, H. Wu, P. Wu, *RSC Adv.* **2018**, *8*, 2751–2758.

[10] a) H. Chen, X. Shi, F. Zhou, H. Ma, K. Qiao, X. Lu, J. Fu, H. Huang, *Catal. Commun.* **2018**, *110*, 102–105; b) G. T. Neumann, J. C. Hicks, *ACS Catal.* **2012**, *2*, 642–646.

[11] L. Meng, X. Zhu, W. Wannapakdee, R. Pestman, M. G. Goesten, L. Gao, A. J. F. van Hoof, E. J. M. Hensen, *J. Catal.* **2018**, *361*, 135–142.

[12] J. H. Lunsford, *Catal. Today* **2000**, *63*, 165–174.

[13] H. Schulz, *Appl. Catal. A* **1999**, *186*, 3–12.

[14] M. Stöcker, *Microporous Mesoporous Mater.* **1999**, *29*, 3–48.

[15] a) H. Koempel, W. Liebner, *Stud. Surf. Sci. Catal.,* **2007**, *167*, 261–267; b) C. J. Maiden, *Stud. Surf. Sci. Catal.* **1988**, *36*, 1–16.

[16] a) D. M. Bibby, R. F. Howe, G. D. McLellan, *Appl. Catal. A* **1992**, *93*, 1–34; b) B. Liu, D. Slocombe, M. AlKinany, H. AlMegren, J. Wang, J. Arden, A. Vai, S. Gonzalez-Cortes, T. Xiao, V. Kuznetsov, *Appl. Petrochem. Res.* **2016**, 6, 209–215..

[17] a) A. Corma, *Chem. Rev.* **1997**, *97*, 2373–2420; b) H. Schulz, *Catal. Today* **2010**, *154*, 183–194; c) F. L. Bleken, K. Barbera, F. Bonino, U. Olsbye, K. P. Lillerud, S. Bordiga, P. Beato, T. V. W. Janssens, S. Svelle, *J. Catal.* **2013**, *307*, 62–73; d) J. Kim, M. Choi, R. Ryoo, *J. Catal.* **2010**, *269*, 219–228.

[18] M. Choi, K. Na, J. Kim, Y. Sakamoto, O. Terasaki, R. Ryoo, *Nature* **2009**, *461*, 246–249.

[19] M. Hartmann, A. G. Machoke, W. Schwieger, *Chem. Soc. Rev.* **2016**, *45*, 3313–3330.

[20] a) F. Meng, Y. Wang, S. Wang, *RSC Adv.* **2016**, *6*, 58586–58593; b) L. Meng, B. Mezari, M. G. Goesten, W. Wannapakdee, R. Pestman, L. Gao, J. Wiesfeld, E. J. M. Hensen, *Catal. Sci. Technol.* **2017**, *7(19)*, 4520–4533; c) M. Milina, S. Mitchell, P. Crivelli, D. Cooke, J. Pérez-Ramírez, *Nat. Commun.* **2014**, *5*, 3922; d) A. A. Rownaghi, J. Hedlund, *Ind. Eng. Chem. Res.* **2011**, *50*, 11872–11878; e) M. Bjørgen, F. Joensen, M. Spangsberg Holm, U. Olsbye, K.-P. Lillerud, S. Svelle, *Appl. Catal. A* **2008**, *345*, 43–50; f) H. Chen, M. Yang, W. Shang, Y. Tong, B. Liu, X. Han, J. Zhang, Q. Hao, M. Sun, X. Ma, *Ind. Eng. Chem. Res.* **2018**, *57*, 10956–10966.

[21] H. Li, Y. Wang, C. Fan, C. Sun, X. Wang, C. Wang, X. Zhang, S. Wang, *Appl. Catal. A* **2018**, *551*, 34–48.

[22] T. Weissenberger, B. Reiprich, A. G. Machoke, K. Klühspies, J. Bauer, R. Dotzel, J. L. Casci, W. Schwieger, *Catal. Sci. Technol.* **2019**, *9*, 3259–3269.

[23] A. G. Machoke, A. M. Beltrán, A. Inayat, B. Winter, T. Weissenberger, N. Kruse, R. Güttel, E. Spiecker, W. Schwieger, *Adv. Mater.* **2015**, *27*, 1066–1070.

[24] a) J. C. Groen, L. A. A. Peffer, J. A. Moulijn, J. Pérez-Ramírez, *Colloids Surf. A* **2004**, *241*, 53–58; b) J. C. Groen, L. A. A. Peffer, J. A. Moulijn, J. Pérez-Ramírez, *Chem. Eur. J.* **2005**, *11*, 4983–4994.

[25] M. Thommes, K. Kaneko, V. Neimark Alexander, P. Olivier James, F. Rodriguez-Reinoso, J. Rouquerol, S. W. Sing Kenneth, *Pure Appl. Chem.,* 1051.

[26] J. C. Groen, J. A. Moulijn, J. Pérez-Ramírez, *Microporous Mesoporous Mater.* **2005**, *87*, 153–161.

[27] J. Pérez-Ramírez, D. Verboekend, A. Bonilla, S. Abelló, *Adv. Funct. Mater.* **2009**, *19*, 3972–3979.

[28] H. Schulz, *Catal. Today* **2010**, *154*, 183–194.

[29] T. Weissenberger, R. Leonhardt, B. A. Zubiri, M. Pitínová-Štekrová, T. L. Sheppard, B. Reiprich, J. Bauer, R. Dotzel, M. Kahnt, A. Schropp, C. Schroer, J.-D. Grunwaldt, J. L. Casci, J. Čejka, E. Spiecker, W. Schwieger, *Chem. Eur. J.* **2019**, *25 (63)*, 14430–14440.

[30] C. Chmelik, M. Liebau, M. Al-Naji, J. Möllmer, D. Enke, R. Gläser, J. Kärger, *ChemCatChem* **2018**, *10(24)*, 5602–5609.